Biomatter 1:1, 91-101; July/August/September 2011; © 2011 Landes Bioscience

Preparation of laminated poly(ε-caprolactone)-gelatin-hydroxyapatite nanocomposite scaffold bioengineered via compound techniques for bone substitution

Azhang Hamlekhan,[1] Fathollah Moztarzadeh,[1] Masoud Mozafari,[1,*] Mahmoud Azami[2] and Nader Nezafati[1]

[1]Biomaterials Group; Faculty of Biomedical Engineering (Center of Excellence); Amirkabir University of Technology; Tehran, Iran; [2]Tissue Engineering and Cell Therapy Department; School of Advanced Medical Technologies; Tehran University of Medical Sciences; Tehran, Iran

Key words: scaffold, poly(ε-caprolactone), gelatin, hydroxyapatite, mesenchymal stem cells, bone substitution

In this research, new bioactive nanocomposite scaffolds were successfully developed using poly(ε-caprolactone) (PCL), cross-linked gelatin and nanoparticles of hydroxyapatite (HAp) after testing different solvents and methods. First, HAp powder was synthesized via a chemical precipitation technique and characterized. Then, the nanocomposites were prepared through layer solvent casting combined with freeze-drying and lamination techniques. According to the results, the increasing of the PCL weight in the scaffolds led to the improvement of the mechanical properties. The amount of ultimate stress, stiffness and also elastic modulus increased from 8 MPa for 0% wt PCL to 23.5 MPa for 50% wt PCL. The biomineralization study revealed the formation of an apatite layer on the scaffolds after immersion in simulated body fluid (SBF). The Ca-P ratios were in accordance to nonstoichiometric biological apatite, which was approximately 1.67. The in vitro biocompatibility and cytocompatibility of the scaffolds were tested using mesenchymal stem cells (MSCs), and the results indicated no sign of toxicity, and cells were found to be attached to the scaffold walls. The in vivo biocompatibility and osteogenesis of these scaffolds in the animal experiments is also under investigation, and the result will be published at the end of the study.

Do not distribute.

Introduction

In the past decade, bone tissue engineering provided new medical therapy as an alternative to conventional transplantation methods using polymeric biomaterials with or without bioactive materials such as bioceramics, bioactive glasses or glass ceramics. In particular, various nanocomposite scaffolds can be fabricated with blends of synthetic and natural polymers by choice of suitable solvents and preparation methods. According to Kim et al.,[1] most synthetic polymers can be modulated with respect to molecular weight, degradation rate and mechanical properties. However, they lack cell recognition sites, and therefore, matrix scaffolds prepared with synthetic polymers often exhibit poor cell adhesion, migration and proliferation. In contrast, most natural polymers show excellent cellular affinity due to the presence of proteins and polysaccharides of extracellular matrix (ECM) components but have poor mechanical properties.

Hence, nanocomposite scaffolds that blend synthetic and natural polymers can exploit the advantages of both polymer types.[2] In addition, applying bioactive materials throughout the nanocomposite scaffold matrices, especially HAp, can drastically improve the bone regeneration ability of these materials. Nowadays, the application potential of scaffolds made from blends of synthetic and natural polymers for tissue regeneration has been investigated by many researchers. For example, composites of PCL and gelatin or collagen were used for tissue engineering applications such as the regeneration of cardiac muscle, skin, nerves and skeletal muscle.[3-7] Although these composite materials exhibit improved cytocompatibility with adjustable mechanical strength, the biopolymer components are often subject to rapid degradation during cell culture or implantation, necessitating physical or chemical cross-linking steps after the fabrication process to covalently link reactive functional groups in biopolymers.[8,9]

Gelatin is a natural biopolymer derived from collagens by controlled hydrolysis.[10,11] Because of its many merits, such as its biological origin, biodegradability, biocompatibility and commercial availability at relatively low cost, gelatin has been widely used in biomedical applications. In pharmaceutical and medical fields, gelatin has long been used as a sealant for vascular prostheses,[12-14] carriers for drug delivery,[15] dressings for wound healing[16] and so forth. Anyway, the approach of mixing gelatin with synthetic polymers has frequently been adopted by other researchers. This is a feasible approach that may not only reduce

*Correspondence to: Masoud Mozafari; Email: mmozafari@aut.ac.ir
Submitted: 04/07/11; Revised: 07/20/11; Accepted: 07/22/11
DOI: 10.4161/biom.1.1.17445

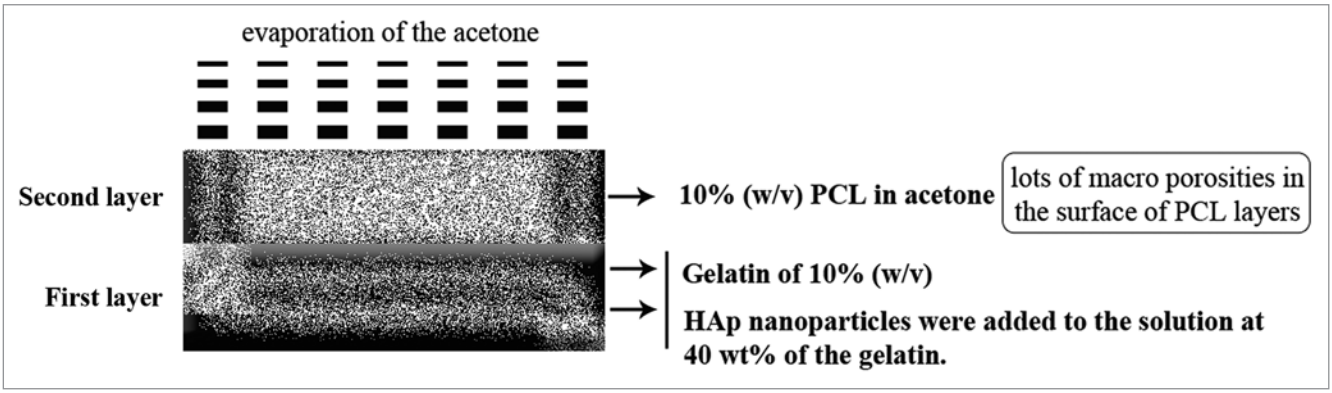

Figure 1. The graphical sketch to describe the preparation procedure of the scaffolds.

the potential problem of cytotoxin as a result of using a chemical cross-linking reagent, but also provide a compromise solution for overcoming the shortcomings of synthetic and natural polymers, that is, producing a new biomaterial with good biocompatibility and improved mechanical and physicochemical properties.

Several nanocomposite scaffolds have been investigated for bone tissue engineering, including HAp, poly(α-hydroxyesters), bioactive glasses and natural polymers, such as gelatin, collagen and chitin. Also, several reviews have been published on the general properties and design features of biodegradable and bioresorbable polymers and scaffolds.[17]

Among synthetic polymers, PCL has been considered an appropriate choice for mixing with gelatin due to the fact that PCL is a semicrystalline linear resorbable aliphatic polyester and has been subjected to hydrolytic degradation because of the susceptibility of its aliphatic ester linkage to hydrolysis.[18-20] On the other hand, PCL is regarded as a soft and hard biocompatible material for tissue engineering applications, such as resorbable suture, drug delivery system and also bone-graft substitutes.[21] Although applications of PCL might be limited because its degradation and resorption kinetics are considerably slower than other aliphatic polyesters, due to its hydrophobic character and high crystallinity, PCL is currently under study for use as a potential material for bone regeneration. Marra et al., in their research on in vitro analysis of biodegradable polymer blend/HAp composites for bone tissue engineering, reported that PCL is a comparable substrate for supporting cell growth resulting from two-dimensional bone marrow stromal cell culture. Moreover, PCL/PLA-blend discs incorporated with HAp are feasible as scaffolding for bone tissue engineering.

From another point of view, applying bioactive ceramics is one of the most famous methods for improving scaffolds for bone repair, and bioactive ceramics based on calcium phosphates (CaP), particularly in the composition of tricalcium phosphate [TCP: $Ca_3(PO_4)_2$] and HAp [$Ca_{10}(PO_4)_6(OH)_2$], have been studied extensively and used clinically.[23-25] The biomaterials research field has focused on the synthesis of these ceramics for three decades for applications in orthopedics and dentistry.[26-32] Previous applications of porous HAp include graft applications in maxillofacial surgery as alveolar ridge augments and as bone defect filler. However, HAp is difficult to handle and keep in defect sites because of its brittleness and low plasticity.[33-38] As mentioned above, each of the materials that has been widely used in the preparation of tissue engineering scaffolds has low mechanical properties, so, for improving this weakness, many works have been accomplished. For example Causa et al. used PCL-based composites with HA particles added at different volume/weight ratios. They showed both good mechanical performance and appreciable biocompatibility. In another work by Chang et al.,[40] gelatin-HAp nanocomposites were fabricated as foams. The mechanical properties of the foams and, in the same research by Lia et al.,[41] the biological and mechanical properties of gelatin-apatite nanofibers were examined, and the result was better than using the gelatin alone, and the scaffolds also showed excellent biocompatibility and mechanical stability.

One of the most important aspects of bone tissue engineering is the introduction of bioactive cells into the scaffolds.[42-46] For the application of MSCs in bone regeneration, understanding the interactions between cells and scaffold materials is particularly important, because the cell-material interaction plays an important role in bonding implant materials to native bone tissue and in preventing the formation of a fibrous capsule. It is obvious that MSCs present more advantages than other cells and have already been widely used in bone tissue engineering.[47-49]

In this study, HAp powder was synthesized by chemical precipitation through aqueous solutions of the reactants. Then, to mimic the mineral and organic component of natural bone, the PCL-Gelatin-HAp nanocomposites were prepared via layer solvent casting combined with freeze-drying and lamination techniques. Finally, glutardialdehyde (GA) was used as a cross-linking agent. The increasing of the PCL weight through the scaffold samples caused the improvement of mechanical properties. Eventually, the cellular responses of the scaffolds were examined. The proliferation of the MSCs in direct contact with the scaffolds was qualitatively determined by Scanning Electron Microscope (SEM) analysis and quantitatively with MTT assay.

Results and Discussion

HAp powder. The XRD data of the nanocrystalline HAp powder is presented in **Figure 2A**. The XRD analysis was performed using an X-ray diffractometer. The straight base line and the

©2011 Landes Bioscience. Do not distribute

Table 1. The best preparation method of the nanocomposite scaffolds

PCL solvent	Gelatin solvent	Method	Result
Acetone	Distilled water	Lamination of PCL layers between gelatin layers	PCL-Gelatin blend was obtained

sharp peaks of the diffractogram confirmed that the product was well crystallized. The XRD patterns indicated that HAp was formed in this sample, and traces of other calcium phosphate impurities were not detected by this technique. The XRD pattern of sintered samples can be completely indexed with HAp in the standard card (JCPDS No. 09-0432), the only phase found present. No processing residue or secondary phases were found in the materials.

Figure 2B shows the FTIR spectrum in the 500–4,000 cm^{-1} spectral range of the HAp powder. The HAp powder exhibited five important infrared bands located at 560, 605, 622, 1,040 and 3,555 cm^{-1}. Among these bands, two bonds were observed at 3,555 and 622 cm^{-1} due to the stretching mode of hydrogen-bonded OH^- ions and the liberational mode of hydrogen-bonded OH^- ions, respectively. In addition, the band at 1,040 cm^{-1} arises from υ_3 PO_4, and the bonds at 605 and 560 cm^{-1} arise from υ_4 PO_4.[50] The FTIR analysis showed all typical absorption characteristics of the HAp powder, and, according to these explanations, it is obvious that the synthesized powder is certainly HAp.

The result of measurement of elemental composition (Ca and P content) and Ca/P molar ratio were chemically analyzed by quantitative chemical analysis via EDTA titration technique and AAS. The Ca and P content and bulk Ca/P molar ratio was determined as 38.63 (wt%), 17.48 (wt%) and 1.71, respectively. The measured Ca/P ratio for this synthesized powder was higher than the stoichiometric ratio (1.667) expected for a pure HAp phase that can arise from local presence of carbonate apatite in which the Ca/P molar ratio can be as high as 3.33.[51]

TEM analysis was used to examine and estimate HAp crystallites. TEM micrographs of the HAp powder in low and high magnifications are shown in **Figure 3**. The crystalline structure of HAp particles has an elliptical shape with a grain size in the range of 8–12 nm.

Nanocomposite scaffolds. *FTIR analyses and chemical bonds.* In order to study the chemical bonds in the nanocomposite scaffolds, FTIR results obtained from two samples were investigated. **Figure 4** shows the FTIR spectra of the samples with 20% wt PCL and 50% wt PCL; the peaks that appeared give information about detected chemical bonds. The FTIR spectra of 20% wt PCL were nearly same as that of 50% wt PCL.

Three series of obtained peaks, like 1,236, 1,450, 1,555, 1,670, 2,930, 3,048 cm^{-1} related to gelatin; peaks at 560, 868, 1,040, 3,558 related to HAp chemical structure, and infrared spectra for PCL-related stretching modes were also observed for both scaffolds, including 2,930, 2,870, 1,670, 1,293 and 1,240 cm^{-1}.[52] But there are two peaks related to chemical bonds that were formed after the mixing of gelatin-HAp and then cross-linking of components, which stood at about 1,345 and 2,363 cm^{-1}, respectively. The first one indicates the formation of a chemical bond between the carboxyl group from gelatin and the Ca^{+2} ion from HAp, which has been mentioned in former studies too.[53,54] Herein, the chemical bonding between HAp nanoparticles and gelatin in the nanocomposites has three major steps:

(1) A critical complex reaction between Ca^{2+} ions of HAp nanoparticles and gelatin molecules.[55,56]

(2) The Ca^{2+} ions the of complex with gelatin molecules assembled with PO_4^{3-} ions from HAp nanoparticles.

(3) The -COOH and -NH_2 groups in the gelatin molecule form chemical bonds with P-O and O-H groups of HAp nanoparticles, resulting in gelatin chains firmly attaching to the surface of HAp nanoparticles.

There are two main sources of stabilization that prevent the occurrence of the HAp particle agglomeration. The first one is electrostatic stabilization and another is spatial stabilization. Here, electrostatic stabilization is mainly due to adsorption of Ca^{2+} ions on the surface of HAp particles. The adsorption would produce an electrical double layer. In other words, the ionization of carboxyl is enforced while that of amino is restrained, and the carboxyl ions of gelatin act, consequently, as counter ions in the electrical double layer. The spatial stabilization in this reaction system is mainly due to chemisorption of gelatin molecules on the HAp particles.[57] Also, the bond at 2,363 cm^{-1} appeared after cross-linking of gelatin with GA. Therefore, this bond arises from the C-H bond in C_3H_6 alkene, which remains in the final cross-linked gelatin chains after GA reaction, as shown:

©2011 Landes Bioscience.
Do not distribute.

$$\text{Gelatin-NH}_2 + \text{C}_5\text{H}_8\text{O}_2 + \text{NH}_2\text{-Gelatin} \rightarrow \text{Gelatin-N = CH - C}_3\text{H}_6\text{ - CH = N = Gelatin}$$

In addition, according to Ghasemi-Mobarakeh et al., PCL and gelatin chains can be chemically bonded. Herein, it is worth mentioning that the appearance of the amide groups in the FTIR spectra of the nanocomposite scaffolds, which is shown with arrows in **Figure 4,** indicates that the PCL chains were chemically bonded to gelatin sidewalls, leading to the introduction of functional groups such as NH_2 and COOH on the surface of prepared scaffolds, which was also reported by former researchers. In conclusion, all these chemical bonds caused a strong and effective structure for the prepared scaffolds.

SEM observations. **Figure 5** shows the morphologies of the PCL, gelatin and nanocomposite layers in different aspects. The morphological analysis of the gelatin layers showed a uniform distribution of pores, with an average size around 150 μm, which is shown in **Figure 5A**. Also, it can be seen that pores are either interconnected or separated via thin walls. During the preparation process, it was expected that the HAp nanoparticles would be distributed homogeneously throughout the gelatin network. The distribution of the HAp nanoparticles is not affected by gravity, because the viscous gelatin was kept in an ultrasonic place and then was rapidly frozen to form a homogeneous nanocomposite layer. According to **Figure 5B and C**, a porous structure is even seen in PCL layers, especially in areas away from the gelatin-PCL

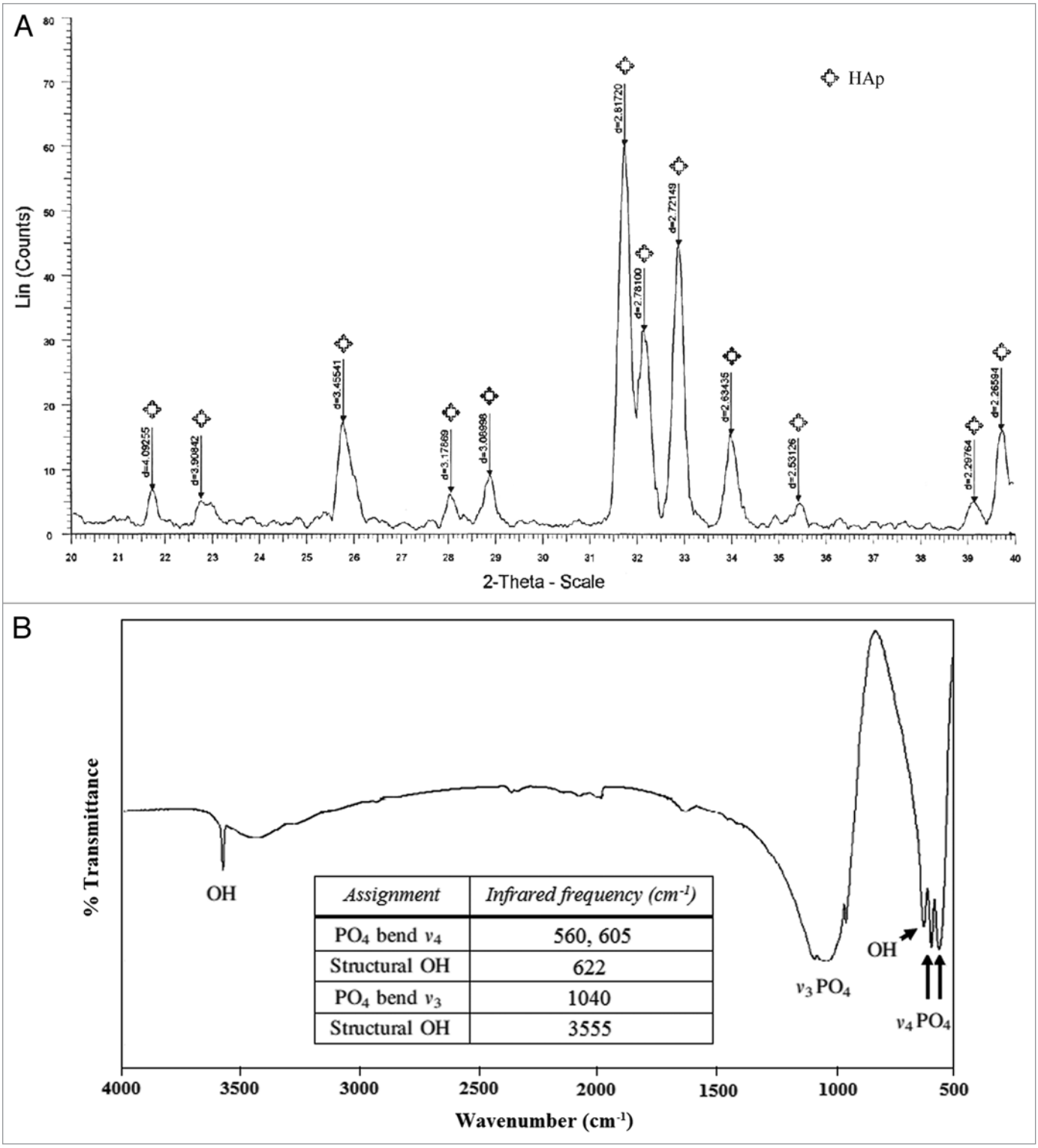

Figure 2. (A) The XRD pattern of the synthesized nanocrystalline HAp powder. (B) The FTIR spectrum of the synthesized HAp powder.

boundary. The pore configurations in the PCL layers are more complex, and the pore size is nearly smaller. It is notable that the PCL and gelatin layers are mechanically bound in most areas to form a gelatin-PCL boundary (see **Fig. 5D and E**). As was mentioned previously, evaporation of acetone during the lamination technique lets macro-pores of the PCL layers make the gelatin layers continuity possible throughout the nanocomposite scaffolds (see **Fig. 5F**).

In vitro biomineralization studies. The in vitro biomineralization of the prepared scaffolds immersed in SBF is shown in

Figure 6. The SEM micrographs showed the deposition of newly formed apatite particles on the surface of the scaffolds. **Figure 6B–D** shows the SEM micrographs of the scaffolds after immersion for 3, 7 and 14 d, respectively. According to these observations, scattered and small particles covered the surface of the scaffolds after 3 d of immersion, which is shown in **Figure 6B**. After 7 d, a substantial amount of apatite microparticles formed on the surfaces (**Fig. 6B**). Also, after 7 d of immersion, the whole inner pore-wall surfaces of the scaffolds were covered by a layer of apatite, and the underlying surfaces were not clearly observable (**Fig. 6D**).

Table 2. Ion concentrations of SBF and human blood plasma[29]

Ion	Plasma (mmol/l)	SBF (mmol/l)
Na^+	142.0	142.0
K^+	5.0	5.0
Mg^{+2}	1.5	1.5
Ca^{+2}	2.5	2.5
Cl^-	103.0	147.8
HCO_3^-	27	4.2
HPO_4^{-2}	1.0	1.0
SO_4^{-2}	0.5	0.5

We also confirmed the formation of apatite layers on the surface of scaffolds by EDX analysis, which is shown in **Figure 6**. The results from EDX analysis revealed the gradual development of the apatite layer on the surfaces and pores of scaffolds after immersion in SBF solution. Furthermore, EDX analysis showed that, after 14 d immersion in SBF solution, the Ca-P ratios were in accordance to nonstoichiometric biological apatite, which was approximately 1.67.

Mechanical properties of the nanocomposite scaffolds. The mechanical properties of the prepared porous scaffolds have been of particular concern for many tissue engineering applications due to the necessity of the structure to withstand stress during culturing in vitro and as in vivo implants. Mechanical properties also influence specific cell functions within the engineered tissues. This is why, in the present study, compressive properties of scaffolds were examined. As can be seen in **Table 3**, increasing the PCL weight caused improvement of the scaffolds' mechanical properties. In addition, the elastic modulus increased from 8 MPa to 23.5 MPa for 50% wt PCL. Also, the amount of ultimate stress and stiffness increased from 1.83 MPa and 38 N/mm to 3.73 MPa and 131 N/mm, respectively. At the same time, a decrease in ultimate strain was observed according to the stress-strain curves.

Biocompatibilty evaluation using MSCs. MSCs represent an attractive and promising field in tissue regeneration and engineering for treatment applications in a wide range of trauma and orthopedic conditions. In the bone tissue engineering field, there has been a special interest in MSCs loaded on scaffolds, which provide a prospective approach for the reconstruction of even large bone defects.[58-60]

In the present study, MSCs derived from the bone marrow of neonatal rabbits were cultured, expanded and seeded on the prepared nanocomposite scaffolds. The proliferation of the MSCs in direct contact with the scaffolds was qualitatively determined with SEM and quantitatively with MTT assay. The biocompatibility of the nanocomposite scaffolds was evaluated in vitro by observing the behavior of the cells cultured in close contact with the scaffolds. According to **Figure 7**, the SEM micrographs of the cells cultured on the surface of nanocomposite scaffolds showed well-spread cells on the scaffolds, an indication of good attachment and penetration to the surface of the scaffolds. It also shows that, after 3 d of cell culturing, the cells with a predominantly fusiform shape attached to the surface of the scaffolds with their pseudopodia. Wide distribution of these traces on the surface of scaffolds is an indication of good cellular migration and osteoconductivity of the scaffolds, and the continuous increase in cell aggregation on the scaffolds during the 3 d incubation also indicated the ability of the scaffolds to support cell growth.

Both the MSCs cultured on the standard plastic plate (control) and MSCs cultured on the nanocomposite scaffolds were evaluated in the osteogenic medium. The cell proliferation in each group was evaluated using MTT test, which is shown in **Figure 8**. In 6-d cell culture, the cell number increased with the culture time in both tested groups. Statistical analysis indicated no significant difference in the cell number between the cells seeded on the scaffold samples and cells cultured on the standard plastic plate in the same osteogenic condition. During the cell culturing in both groups, the number of cells grew dramatically. This similar ascendant tendency of the cell population demonstrated that the nanocomposite scaffolds have little influence on cell growth.

According to the results, we came to the conclusion that the prepared nanocomposite scaffolds have no negative effect on the attachment and proliferation of MSCs, and they are in vitro biocompatible and noncytotoxic to cells.

©2011 Landes Bioscience. Do not distribute.

Materials and Methods

Materials. Calcium nitrate tetra-hydrate [$Ca(NO_3)_2$ $0.4H_2O$, 98%], di-ammonium hydrogen phosphate [$(NH4)_2HPO_4$, 99%] and sodium hydroxide [NaOH, 99%] were purchased from Merck Inc. to synthesize the HAp powder by precipitation technique. PCL used in this study were obtained from Solvay, with an average molecular weight of 50,000 (CAPA-6500). Also, gelatin for microbiology (Merck No. 104070) was used. The gelatin foams were cross-linked by immersing into Glutardialdehyde (Merck No. 820603). Distilled water, acetone extra pure, Dimethyl sulfoxide (DMSO), tetrahydrofuran (THF), N,N-Dimethylformamide (DMF) and acetic acid 100% (glacial) were used as polymer solvents.

Synthesis of nanocrystalline HAp powder. The HAp powder was prepared by chemical precipitation through aqueous solutions of the reactants. A total of 0.09 M diammonium hydrogen phosphate solution and 0.15 M calcium nitrate tetrahydrate solution were prepared, and the pH of the both solutions was brought

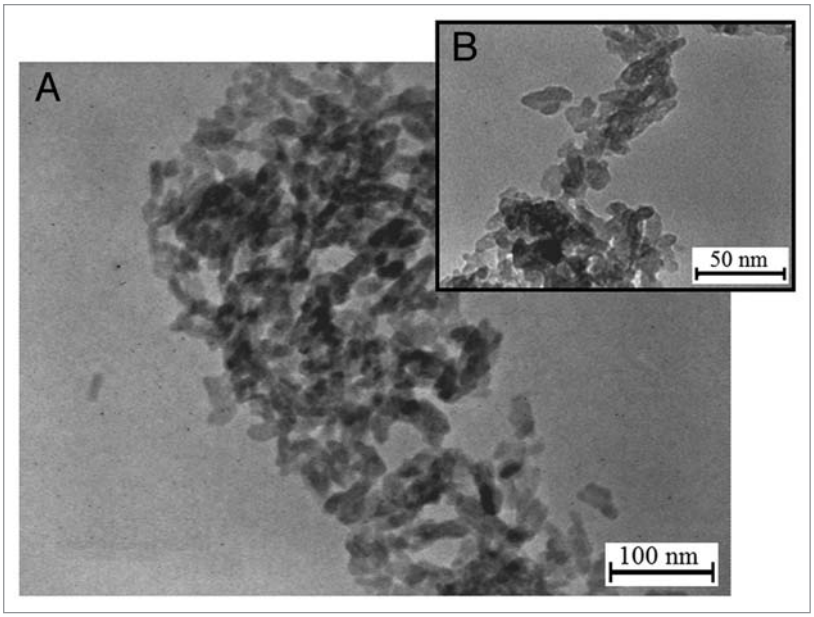

Figure 3. The TEM micrographs of the HAp powder, (A) low and (B) high magnifications.

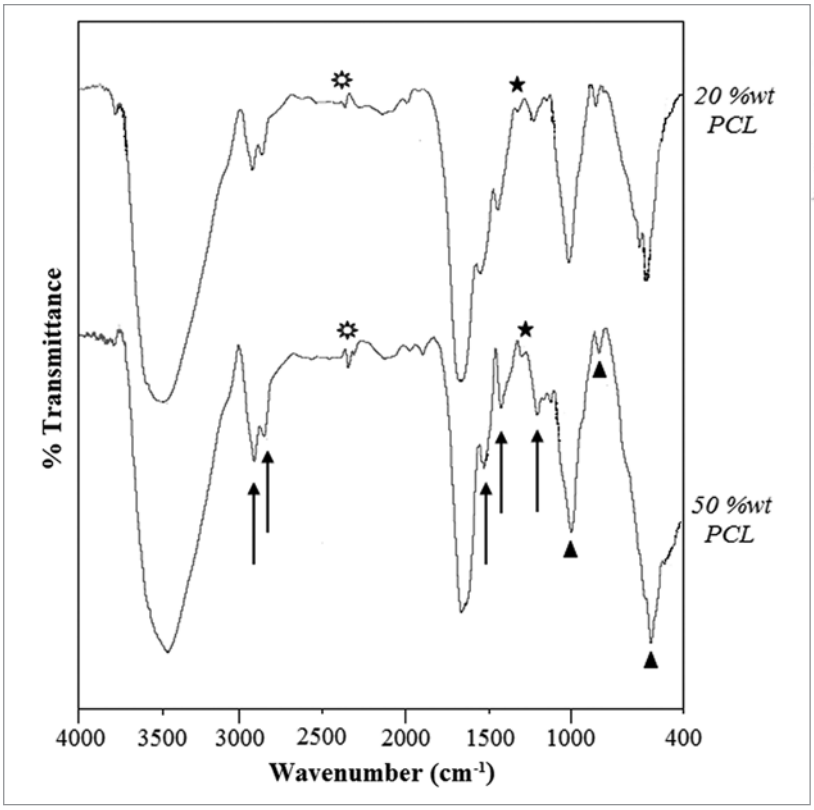

Figure 4. The FTIR spectra of the nanocomposite samples with 20% wt PCL (top) and 50% wt PCL (bottom). Triangles, Hap; stars, 1,345 (cm^{-1}) related to the gelatin-HAp bond; sunbursts, 2,363 (cm^{-1}) related to the cross-linking process.

to 10 by adding a small amount of sodium hydroxide solution. The phosphate solution was added drop-wise into the calcium nitrate solution, resulting in the precipitation of HAp. The precipitation of HAp can be described by the following reactions (1) and/or (2):[61]

$$10\ Ca^{+2} + 6\ H_2PO_4^- + 2\ OH^- \rightarrow Ca_{10}(PO_4)_6(OH)_2 + 6\ H^+ \quad (1)$$

$$10\ Ca^{+2} + 6\ H_2PO_4^- + 2\ OH^- \rightarrow Ca_{10}(PO_4)_6(OH)_2 + 12\ H^+ \quad (2)$$

After ripening for a specified period of time (24 h) at room temperature, the precipitates were recovered by centrifuge and then washed with deionized water. Five cycles of washing and centrifuging were repeated to ensure complete removal of the by-product. The calcination of the synthesized powders was performed at 800°C for 1 h in air using a heating rate at 3.0°C/min in an electrical tube furnace from room temperature to 800°C after drying the sample in freeze-drier for 10 h.

Preparation of the nanocomposite scaffolds. The gelatin of 10% (w/v) was added into distilled water and stirred at 40°C for 1 h. HAp nanoparticles were added to the solution at 40 wt% of the gelatin. The mixture was homogenized in an ultrasonic place by a stirrer at 40°C for 1 h. The gelatin-HAp solution was poured into plastic dishes and left in ambient conditions for 10 min to form the first gelatin-HAp layer. Then, as can be seen in **Table 1**, a solution of 10% (w/v) PCL in acetone was poured on the gelatin-HAp layer, and the complex was left in ambient conditions for 20 min to form the PCL layer. After evaporation of the acetone, the gelatin-HAp solution was poured again to fabricate the next gelatin-HAp layer. Lamination was continued to form the fourth gelatin-HAp layer. After evaporation of the acetone, lots of macro-porosities were observed in the surface of PCL layers, which made gelatin able to influence all the nanocomposite layers. Five samples were prepared in which PCL amounts were 0, 20, 30, 40 and 50 wt% of gelatin. The samples were frozen in the freezer at -20°C for 24 h and then moved to the freeze-drier for 72 h. To cross-link gelatin polymeric chains and to reduce biodegradation and enhance the biomechanical properties of the scaffolds for tissue repair, the prepared samples were immersed into 1% glutardialdehyde aqueous solution for 24 h to cross-link the gelatin-HAp layers. Finally, the cross-linked nanocomposite scaffolds were carefully washed several times to remove the rest of GA and then dried at room temperature. The graphical sketch of the preparation procedure of scaffolds is presented in **Figure 1**.

Table 3. The mechanical properties of the nanocomposite scaffolds

Samples	0% wt PCL	20% wt PCL	30% wt PCL	40% wt PCL	50% wt PCL
$E_{0.02}$ (MPa)	8 ± 1.2	16 ± 3.3	19 ± 1.6	20.5 ± 1.3	23.5 ± 4.8
G_{ult} (Mpa)	1.83 ± 0.5	3.13 ± 0.4	3.40 ± 0.1	3.71 ± 1.1	3.73 ± 1
K (N/mm)	38 ± 2	79 ± 4.1	93 ± 3.9	114 ± 2.7	131 ± 7.1

Preparation of SBF solution. The SBF solution was prepared by dissolving reagent-grade NaCl, KCl, $NaHCO_3$, $MgCl_2.6H_2O$, $CaCl_2$ and KH_2PO_4 into distilled water and buffered at pH = 7.25 with TRIS (trishydroxymethyl aminomethane) and HCl 1 N at 37°C. Its composition is given in **Table 2** and is compared with the human blood plasma as previously described by Mozafari et al.[29]

Characterization. *HAp powder characterization.* The resulting powder was analyzed by X-ray diffraction (XRD) with a Siemens-Brucker D5000 diffractometer. This instrument works with voltage and current settings of 40 kV and 40 mA, respectively and uses Cu-Kα radiation (1.540600 Å). For qualitative analysis, XRD diagrams were recorded in the interval $20 \leq 2\theta \leq 60°$ at a scan speed of 2°/min, 0.02° being the step size and 1 sec being the step time.

The HAp sample was examined by Fourier transform infrared spectroscopy with a Bomem MB 100 spectrometer. For IR analysis, first 1 mg of the powder sample was carefully mixed with 300 mg of KBr (infrared grade) and pelletized under vacuum. Then, the pellet was analyzed in the range of 500–4,000 cm^{-1} at a scan speed of 23 scan/min with 4 cm^{-1} resolution.

In order to calculate the Ca/P molar ratio of the precipitated powder, the content of Ca and P were chemically analyzed by quantitative chemical analysis via EDTA titration technique and atomic absorption spectroscopy (AAS) with a Shimadzu UV-31005 instrument, respectively.

Transmission electron microscopy (TEM; CM200-FEG-Philips) was used for characterizing the particles. For this purpose, particles were deposited onto Cu grids, which supported a carbon film. The particles were deposited onto the support grids by deposition from a dilute suspension in acetone or ethanol. The particles' shape and size were characterized by diffraction (amplitude) contrast and, for crystalline materials, by high-resolution (phase contrast) imaging.

Nanocomposite scaffolds characterization. The functional groups of nanocomposite samples were ascertained by Fourier transform infrared spectroscopy (FTIR). For IR analysis, first samples were powdered and then dispersed into pellets of KBr (infrared grade) and the spectra recorded by Bomem MB 100 spectrometer in the range 400–4,000 cm^{-1} at a scan speed of 23 scan/min with 4 cm^{-1} resolution.

Microstructure and morphology of porous nanocomposite (pore morphology) and measurement of pore size were evaluated using SEM analysis. For this purpose, the nanocomposite samples were coated with a thin layer of Gold (Au) by sputtering (EMITECH K450X, England), and then the morphology of the samples were observed on a scanning electron microscope (SEM-Philips XL30) that operated at the acceleration voltage of 15 kV. An energy dispersive X-ray analyzer (EDX, Rontec, Germany) directly connected to SEM was used to investigate semi-quantitatively chemical compositions.

Compression strength tests were performed on the porous foams. Each sample was loaded using Zwick-Roell (MCT-25-400, Germany) at a crosshead speed of 2 mm/min with a load of 500 N cell in ambient conditions. The stress-strain curve was obtained to determine mechanical properties, including elastic modulus, compression strength, maximum stress and strain at maximum stress. The elastic modulus was obtained from the slope at the initial stages of loading (2% strain). Five specimens were tested for each composite.

Porosity measurement. Pore volume (Vp) was calculated according to the following equation:

$$Vp = Vsk - VBG - VGel = Vsk - (WBG/\rho BG) - (WGel/\rho Gel)$$

where Vsk is the skeletal volume of the nanocomposite (cm^3), VBG the actual volume of BaG (cm^3) and VGel the actual volume of gelatin (cm^3); in addition, VBG and VGel were measured with attention to the mass and the density of BaG and gelatin, which were used in each sample. The density of BaG and gelatin are ρ = 2.7 and ρ = 1.35, respectively. So, the calculation formula of porosity (%) is defined as follows:

$$\text{porosity (\%)} = (Vp/Vsk) \times 100$$

©2011 Landes Bioscience. Do not distribute.

In vitro biomineralization studies. Three scaffolds of equal weight and shape were immersed in SBF solution and incubated at 37°C in a closed Falcon tube for 3, 7 and 14 d. After the specified times, the scaffolds were removed and then carefully washed four times with deionized water to remove adsorbed minerals. Finally, the scaffolds were lyophilized, viewed and analyzed using SEM and EDX for mineralization.

In vitro cell attachment and proliferation. *MSCs seeding.* First, MSCs were aspirated from the bone marrow of neonatal rabbits, gradient centrifuged and plated into flasks containing Dulbecco's modified Eagle's medium low glucose containing 10% fetal bovine serum and 2% antibiotics (200 μg/ml penicillium and 200 μg/ml streptomycin). MSCs at passage three were removed into the culture medium containing osteogenic factors (50 μg/l α-ascorbic acid, 10-8 mol/l dexamethasone and 10 mmol/l β-glycerophosphate, 10 mmol/l VitD3, 100 μg/ml penicillium and 100 μg/ml streptomycin, 0.3 μg/m amphotericin, 2.2 g/l sodium bicarbonate and 15% fetal bovine serum). Medium was changed every 3 d.

Then, the prepared nanocomposite scaffolds were sterilized by ethylene oxide gas and presented in the osteogenic culture medium for 24 h. MSCs that were cultured in osteogenic medium for 1 week were seeded onto the tops of the pre-wetted

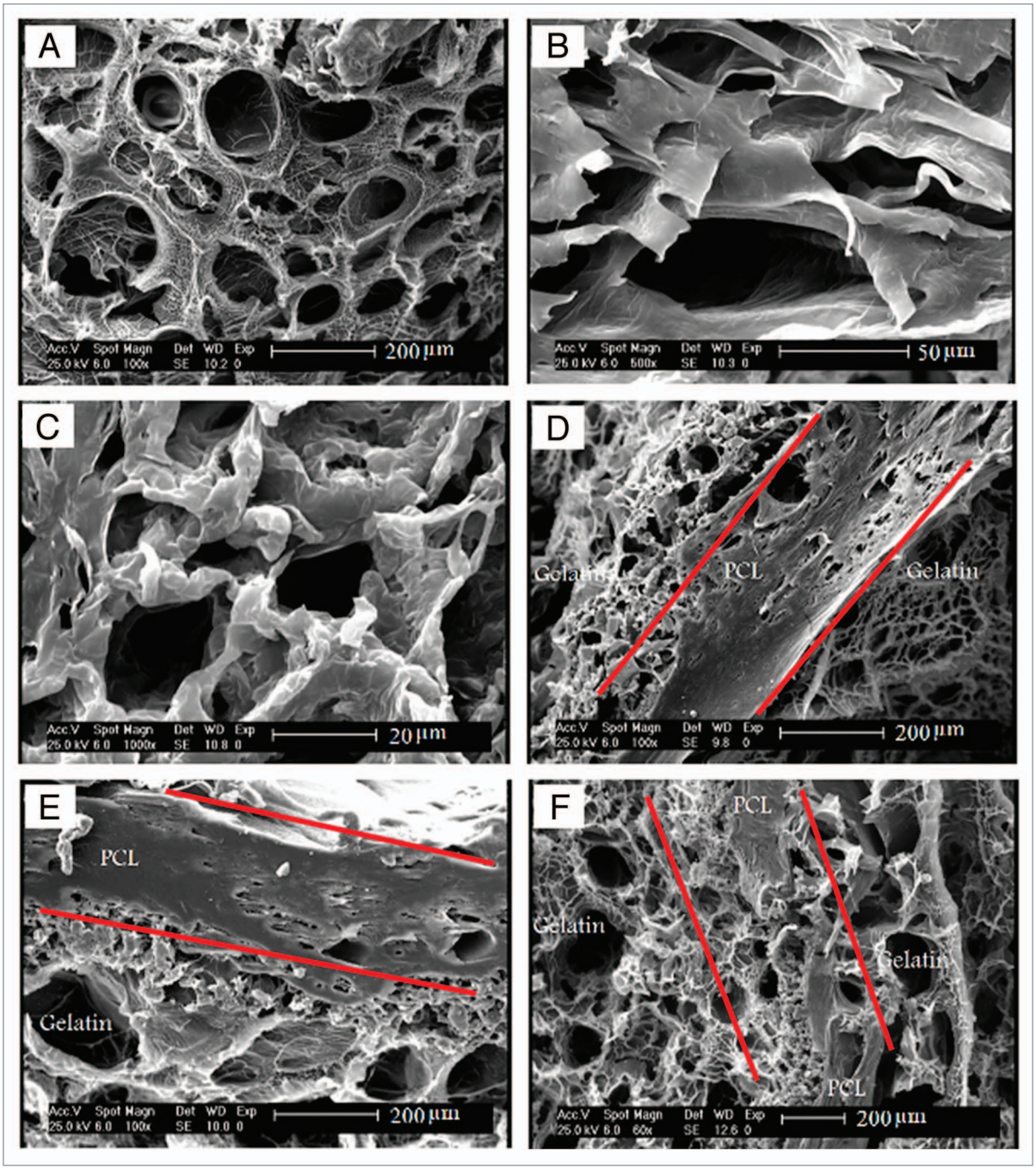

Figure 5. The SEM micrographs of (A) the gelatin layer in the nanocomposite containing 20% wt PCL, (B) the PCL layer in the nanocomposite containing 20% wt PCL, (C) the PCL layer in the nanocomposite containing 50% wt PCL, (D) the gelatin-PCL boundary in the nanocomposite containing 20% wt PCL, (E) the gelatin-PCL boundary in nanocomposite containing 50% wt PCL and (F) the continuity of the gelatin layers in the nanocomposite containing 20% wt PCL.

scaffolds (2.0 x 10^6 cells/scaffold), and then the scaffold/cell constructs were placed in the wells of tissue culture plates. The scaffolds were left undisturbed in an incubator for 3 h to allow the cells to attach to them, and then an additional 1 ml of culture medium was added into each well. The cell/scaffold constructs were cultured in a humidified incubator at 37°C with 95% air and 5% CO_2 for 7 d. The medium was changed every 3 d.

MTT assay. The proliferation of MSCs on the nanocomposite scaffolds was determined using the MTT assay. Thus, MSCs were cultured on the nanocomposite scaffolds for 1, 3 and 6 d, and their proliferation rates were compared with the cells cultured on standard plastic culture surfaces. For this purpose, six samples were prepared in each group. The test was performed according to the manufacturer's (Sigma) instructions, and the

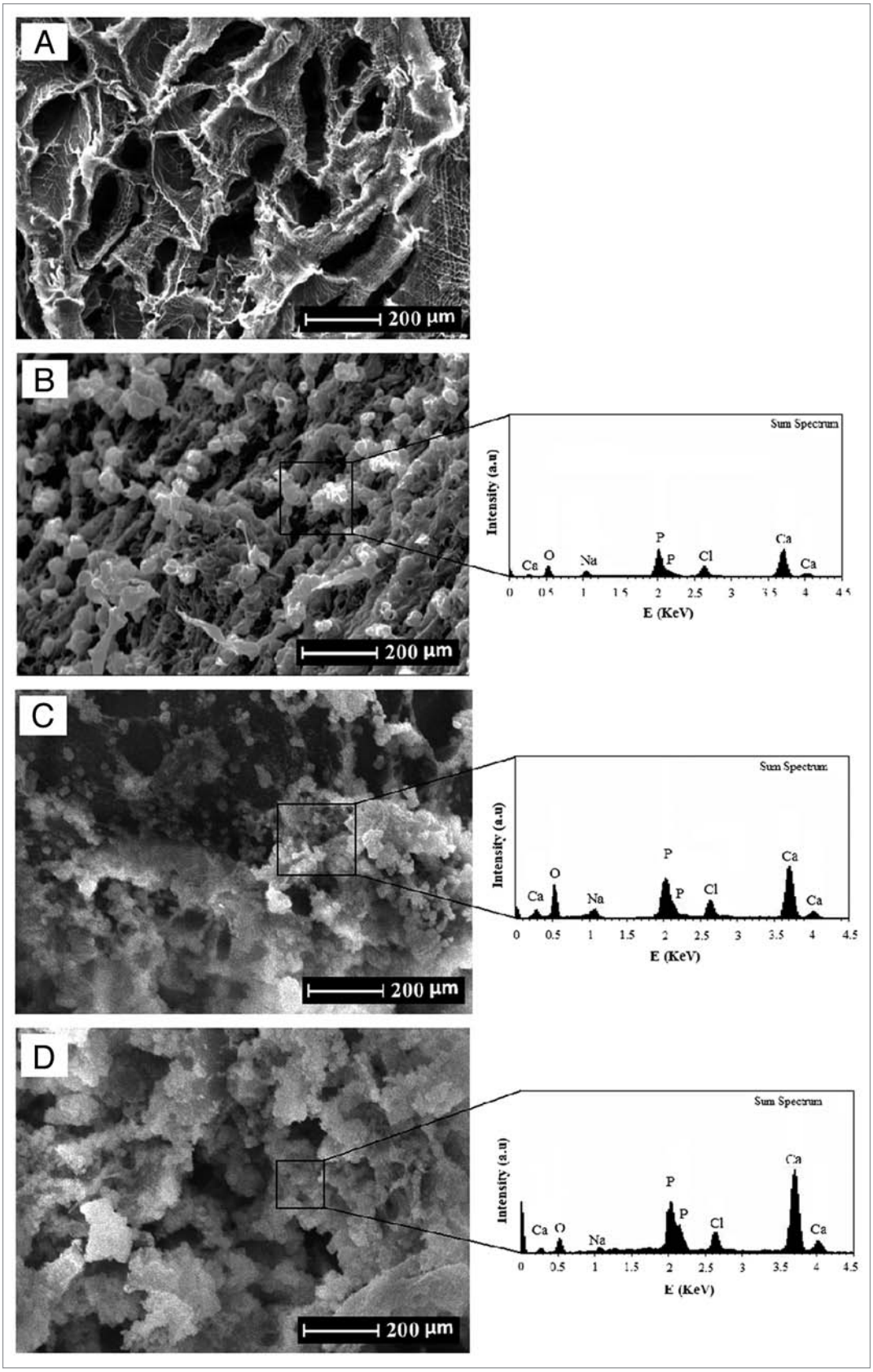

Figure 6. The SEM micrographs of the nanocomposite scaffolds before and after immersion in SBF (A) before immersion, (B) 3 d, (C) 7 d and (D) 14 d.

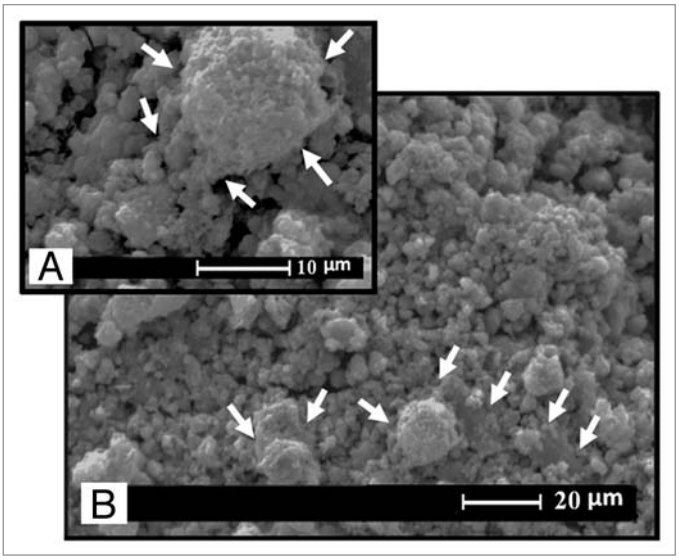

Figure 7. The SEM micrographs of the MSCs cultured on the surface of the nanocomposite scaffolds.

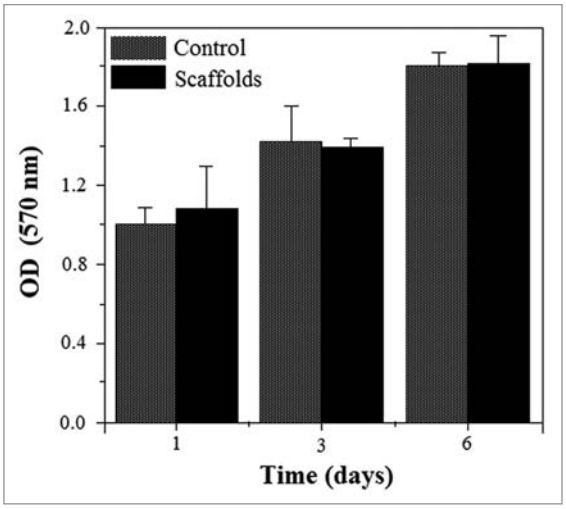

Figure 8. The MTT cell proliferation on the standard plastic plate (control) and scaffolds showing biocompatibility of the nanocomposite scaffolds.

colorimetry was performed at 570 nm. A blank OD value was reduced from each sample's reading.

Statistical analysis. All experiments were performed in fifth replicate. The results were given as means ± standard error (SE). Statistical analysis was performed by using one-way ANOVA and Tukey test, with significance reported when $p < 0.05$. Also for investigation of group normalizing, Kolmogorov-Smirnov test was used.

©2011 Landes Bioscience. Do not distribute.

Conclusion

In this study, after testing different solvents and preparation methods, the novel PCL-gelatin-HAp nanocomposite scaffolds were successfully prepared using a new effective lamination technique. The chemical bonds between gelatin and HAp and also between gelatin and PCL made it mechanically effective. The nanocomposite scaffolds were macroporous in nature, and pore size ranged from 150 to 500 µm. The results from biomineralization studies revealed the gradual development of the apatite layer on the surfaces and pores of scaffolds after immersion in SBF. Furthermore, EDX analysis showed that, after 14 d immersion in SBF solution, the Ca-P ratios were in accordance to nonstoichiometric biological apatite, which was approximately 1.67. The in vitro biocompatibility results showed that the scaffolds were biocompatible, and MSCs seeded on the scaffolds attached to the pore walls. Therefore, we concluded that the PCL-gelatin-HAp nanocomposite scaffold could be used as an appropriate alternative for bone tissue engineering applications.

Disclosure of Potential Conflicts of Interest

No potential conflicts of interest were disclosed.

References

1. Kim MS, Jun I, Shin YM, Jang W, Kim SI, Shin H. Heungsoo Shin, The development of genipin-cross-linked poly(caprolactone) (PCL)/gelatin nanofibers for tissue engineering applications. Macromol Biosci 2010; 10:91-100; PMID:19685497; DOI:10.1002/mabi.200900168.
2. Barnes CP, Sell SA, Boland ED, Simpson DG, Bowlin GL. Nanofiber technology: Designing the next generation of tissue engineering scaffolds. Adv Drug Deliv Rev 2007; 59:1413-33; PMID:17916396; DOI:10.1016/j.addr.2007.04.022.
3. Blackwood KA, McKean R, Canton I, Freeman CO, Franklin KL, Cole D, et al. Development of bio-degradable electrospun scaffolds for dermal replacement. Biomaterials 2008; 29:3091-104; PMID:18448164; DOI:10.1016/j.biomaterials.2008.03.037.
4. Choi JS, Lee SJ, Christ GJ, Atala A, Yoo JJ. The influence of electrospun aligned poly(varepsilon-caprolactone)/collagen nanofiber meshes on the formation of self-aligned skeletal muscle myotubes. Biomaterials 2008; 29:2899-906; PMID:18400295; DOI:10.1016/j.biomaterials.2008.03.031.
5. Ghasemi-Mobarakeh L, Prabhakaran MP, Morshed M, Nasr-Esfahani MH, Ramakrishna S. Electrospun poly(3-caprolactone)/gelatin nanofibrous scaffolds for nerve tissue engineering. Biomaterials 2008; 29:4532-9; PMID:18757094; DOI:10.1016/j.biomaterials.2008.08.007.
6. Heydarkhan-Hagvall S, Schenke-Layland K, Dhanasopon AP, Rofail F, Smith H, Wu BM, et al. Three-dimensional electrospun ECM-based hybrid scaffolds for cardiovascular tissue engineering. Biomaterials 2008; 29:2907-14; PMID:18403012; DOI:10.1016/j.biomaterials.2008.03.034.
7. Zong X, Bien H, Chung CY, Yin L, Fang D, Hsiao BS, et al. Electrospun fine-textured scaffolds for heart tissue constructs. Biomaterials 2005; 26:5330-8; PMID:15814131; DOI:10.1016/j.biomaterials.2005.01.052.
8. Schiffman JD, Schauer CL. Cross-Linking Chitosan Nanofibers Biomacromolecules. Biomacromolecules 2007; 8:594-601; PMID:17291083; DOI:10.1021/bm060804s.
9. Ye P, Xu ZK, Wu J, Innocent C, Seta P. Nanofibrous Membranes Containing Reactive Groups: Electrospinning from Poly(acrylonitrile-co-maleic acid) for Lipase Immobilization. Macromolecules 2006; 39:1041-5; DOI:10.1021/ma0517998.
10. Rose PI. In: Mark HF, Bikales NM, Overberger CG, Menges G, Kroschwitz JI, Editors. Encyclopedia of polymer science and engineering, New York: Wiley 1987; 488.
11. Johns P, Courts A. In: Ward AG, Courts A, Editors. The science and technology of gelatin, London: Academic 1977; 138.
12. Guidoin R, Marceau D, Rao TJ, King M, Merhi Y, Roy PE, et al. In vitro and in vivo characterization of an impervious polyester arterial prosthesis: The Gelseal Triaxial_graft. Biomaterials 1987; 8:433-41; PMID:3427141; DOI:10.1016/0142-9612(87)90079 2.
13. Jonas RA, Ziemer G, Schoen FJ, Britton L, Castaneda AR. A new sealant for knitted Dacron prostheses minimally cross-linked gelatin. J Vasc Surg 1988; 7:414-9; PMID:2450210.
14. Marois Y, Chakfe¥ NL, Deng X, Marois M, How T, King MW, et al. Carbodiimide cross-linked gelatin: a new coating for porous polyester arterial prostheses. Biomaterials 1995; 16:1131-9; PMID:8562788; DOI:10.1016/0142-9612(95)93576-Y.
15. Tabata Y, Hijikata S, Ikada Y. Enhanced vascularization and tissue granulation by basic fibroblast growth factor impregnated in gelatin hydrogels. J Control Release 1994; 31:189-99; DOI:10.1016/0168-3659(94)00035-2.

16. Ulubayram K, Cakar AN, Korkusuz P, Ertan C, Hasirci N. EGF containing gelatin-based wound dressings. Biomaterials 2001; 22:1345-56; PMID:11336307; DOI:10.1016/S0142-9612(00)00287-8.
17. Schnettler R, Alt V, Dingeldein E, Pfefferle HJ, Kilian O, Meyer C, et al. Bone ingrowth in bFGF-coated hydroxyapatite ceramic implants. Biomaterials 2003; 24:4603-8; PMID:12951003; DOI:10.1016/S0142-9612(03)00354-5.
18. Bezwada RS, Jamiolkowski DD, Lee I, Vishvaroop A, Persivale J, Treka-Benthin S, et al. a new ultra-pliable absorbable monofilament suture. Biomaterials 1995; 16:1141-8; PMID:8562789; DOI:10.1016/0142-9612(95)93577-Z.
19. Darney PD, Monroe SE, Klaisle CM, Alvarado A. Clinical evaluation of the Capronor contraceptive implant—preliminary report. Am J Obstet Gynecol 1989; 160:1292-5; PMID:2497647.
20. Rohner D, Hutmacher DW, Cheng TK, Oberholzer M, Hammer B. In vivo efficacy of bone-marrow-coated polycaprolactone scaffolds for the reconstruction of orbital defects in the pig. J Biomed Mater Res B 2003; 66:574-80; PMID:12861610; DOI:10.1002/jbm.b.10037.
21. Kweon H, Yoo MK, Park IK, Kim TH, Lee HC, Lee HS, et al. A novel degradable polycaprolactone network for tissue engineering. Biomaterials 2003; 24:801-8; PMID:12485798; DOI:10.1016/S0142-9612(02)00370-8.
22. Marra KG, Szem JW, Kumta PN, DiMilla PA, Weiss LE. In vitro analysis of biodegradable polymer blend/hydroxyapatite composites for bone tissue engineering. J Biomed Mater Res 1999; 47:324-35; PMID:10487883; DOI:10.1002/(SICI)1097-4636(19991205)47:3<324::AID-JBM6>3.0.CO;2-Y.
23. Jones F. Teeth and bones: Applications of surface science to dental materials and related biomaterials. Surf Sci Rep 2001; 42:75-205; DOI:10.1016/S0167-5729(00)00011-X.
24. Kikuchi M, Itoh S, Ichinose S, Shinomiya K, Tanaka J. Self-organization mechanism in a bonelike hydroxyapatite/collagen nanocomposite synthesized in vitro and its biological reaction in vivo. Biomaterials 2001; 22:1705-11; PMID:11396873; DOI:10.1016/S0142-9612(00)00305-7.
25. Liou SC, Chen SY, Liu DM. Synthesis and characterization of needlelike apatitic nanocomposite with controlled aspect ratios. Biomaterials 2003; 24:3981-8; PMID:12834593; DOI:10.1016/S0142-9612(03)00303-X.
26. Poursamar SA, Azami M, Mozafari M. Controllable synthesis and characterization of porous polyvinyl alcohol/hydroxyapatite nanocomposite scaffolds via an in situ colloidal technique. Colloids Surf B Biointerfaces 2011; 84:310-6; PMID:21310596; DOI:10.1016/j.colsurfb.2011.01.015.
27. Hamlekhan A, Mozafari M, Nezafati N, Azami M, Hadipour H. A proposed fabrication method of novel PCL-GEL-HAp nanocomposite scaffolds for bone tissue engineering applications. Adv Compos Lett 2010; 19:123-30.
28. Azami M, Jalilifiroozinezhad S, Mozafari M. Synthesis and solubility of calcium fluoride/hydroxy-fluorapatite nanocrystals for dental applications. Ceram Int 2011; 37:2007-14; DOI:10.1016/j.ceramint.2011.02.025.
29. Mozafari M, Rabiee M, Azami M, Maleknia S. Biomimetic formation of apatite on the surface of porous gelatin/bioactive glass nanocomposite scaffolds. Appl Surf Sci 2010; 257:1740-9; DOI:10.1016/j.apsusc.2010.09.008.
30. Razavi A, Moztarzadeh F, Mozafari M, Azami M, Baghbani F. Synthesis and characterization of high-pure nanocrystalline forsterite and its potential for soft tissue applications. Adv Compos Lett 2011; 20:41-7.
31. Sepahvandi A, Moztarzadeh F, Mozafari M, Ghaffari M, Raee N. Photoluminescence in the characterization and early detection of biomimetic bone-like apatite formation on the surface of alkaline-treated titanium implant: State of the art. Colloids Surf B Biointerfaces 2011; 86:390-6; PMID:21592746; DOI:10.1016/j.colsurfb.2011.04.027.
32. Nezafati N, Moztarzadeh F, Hesaraki S, Mozafari M. Synergistically reinforcement of a self-setting calcium phosphate cement with bioactive glass fibers. Ceram Int 2010; 37:927-34; DOI:10.1016/j.ceramint.2010.11.002.
33. Peng J, Li X, Guo G, Yi T, Fu S, Liang H, et al. Preparation and Characterization of Poly(vinyl alcohol)/Poly(caprolactone)-Poly(ethylene glycol)-Poly(caprolactone)/Nano-Hydroxyapatite Composite Membranes for Tissue Engineering. J Nanosci Nanotechnol 2011; 11:2354-60; PMID:21449393; DOI:10.1166/jnn.2011.3139.
34. Tyagi P, Catledge SA, Stanishevsky A, Thomas V, Vohra YK. Nanomechanical Properties of Electrospun Composite Scaffolds Based on Polycaprolactone and Hydroxyapatite. J Nanosci Nanotechnol 2009; 9:4839-45; PMID:19928159; DOI:10.1166/jnn.2009.1588.
35. Sadjadi MAS, Meskinfam M, Sadeghi B, Jazdarreh H, Zare K. In Situ Biomimetic Synthesis and Characterization of Nano Hydroxyapatite in Gelatin Matrix. J Biomed. Nanotechnol 2011; 7:450-4.
36. Sadjadi MAS, Jazdarreh H, Zare K. Biocompatibility Evaluation of Nano Hydroxyapatite-Starch Biocomposites M. Meskinfam. J Biomed Nanotechnol 2011; 7:455-9.
37. Sahithi K, Swetha M, Prabaharan M, Moorthi A, Saranya N, Ramasamy K, et al. Synthesis and Characterization of Nanoscale-Hydroxyapatite-Copper for Antimicrobial Activity Towards Bone Tissue Engineering Applications. J Biomed. Nanotechnol 2010; 6:333-9; PMID:21323106; DOI:10.1166/jbn.2010.1138.
38. Zeng S, Fu S, Guo G, Liang H, Qian Z, Tang X, et al. Preparation and Characterization of Nano-Hydroxyapatite/Poly(vinyl alcohol) Composite Membranes for Guided Bone Regeneration. J Biomed Nanotechnol 2011; 7:549-57.
39. Causa F, Netti PA, Ambrosio L, Ciapetti G, Baldini N, Pagani S, et al. Poly-α-caprolactone/hydroxyapatite composites for bone regeneration: in vitro characterization and human osteoblast response. J Biomed Mater Res A 2006; 76:151-9; PMID:16258959; DOI:10.1002/jbm.a.30528.
40. Chang MC, Ko CC, Douglas WH. Preparation of hydroxyapatite-gelatin nanocomposite. Biomaterials 2003; 24:2853-62; PMID:12742723; DOI:10.1016/S0142-9612(03)00115-7.
41. Liu X, Smith LA, Hu J, Maa PX. Biomimetic nanofibrous gelatin/apatite composite scaffolds for bone tissue engineering. Biomaterials 2009; 30:2252-8; PMID:19152974; DOI:10.1016/j.biomaterials.2008.12.068.
42. Zhang Y, Ouyang H, Lim CT, Ramakrishna S, Huang ZM. Electrospinning of gelatin fibers and gelatin/PCL composite fibrous scaffolds. J Biomed Mater Res B Appl Biomater 2004; 72:156-63; PMID:15389493; DOI:10.1002/jbm.b.30128.
43. Majumdar MK, Keane-Moore M, Buyaner D, Hardy WB, Moorman MA, Mclntosh KR. Characterization and functionality of cell surface molecules on human mesenchymal stem cells. J Biomed Sci 2003; 10:228-41; PMID:12595759; DOI:10.1007/BF02256058.
44. Sun JS, Tsuang YH, Liao CJ, Liu HC, Hang YS, Lin FH. The effects of calcium phosphate particles on the growth of osteoblasts. J Biomed Mater Res 1997; 37:324-34; PMID:9368137; DOI:10.1002/(SICI)1097-4636(19971205)37:3<324::AID-JBM3>3.0.CO;2-N.
45. Murphy WL, Hsiong S, Richardson TP, Simmons CA, Mooney DJ. Effects of a bone-like mineral film on phenotype of adult human mesenchymal stem cells in vitro. Biomaterials 2005; 26:303-10; PMID:15262472; DOI:10.1016/j.biomaterials.2004.02.034.
46. Kasten P, Luginbuhl R, van Griensven M, Barkhausen T, Krettek C, Bohner M. Comparison of human bone marrow stromal cells seeded on calcium-deficient hydroxyapatite, beta-tricalcium phosphate and demineralized bone matrix. Biomaterials 2003; 24:2593-603; PMID:12726713; DOI:10.1016/S0142-9612(03)00062-0.
47. Wang H, Li Y, Zuo Y, Li J, Ma S, Cheng L. Biocompatibility and osteogenesis of biomimetic nano-hydroxyapatite/polyamide composite scaffolds for bone tissue engineering. Biomaterials 2007; 28:3338-48; PMID:17481726; DOI:10.1016/j.biomaterials.2007.04.014.
48. Salgada AJ, Coutinho OP, Reis RL. Bone tissue engineering: state of the art and future trends. Macromol Biosci 2004; 4:743-65; PMID:15468269; DOI:10.1002/mabi.200400026.
49. Martin BJ, Pittenger MF. Bone marrow-derived stem cell for myocardial regeneration: preclinical experience, In: Nabil D, Taylor DA, Diethrich EB, Editors. Stem cell therapy and tissue engineering for cardiovascular repair from basic research to clinical applications, USA: Springer US 2006; 137-57.
50. Rameshbabu N, Kumar TSS, Prasad Rao K. Synthesis of nanocrystalline fluorinated hydroxyapatite by microwave processing and its in vitro dissolution study. Bull Mater Sci 2006; 29:611-5; DOI:10.1007/s12034-006-0012-3.
51. Wei M, Evans JH, Bostrom T, Grondahl L. Synthesis and characterization of hydroxyapatite, fluoride-substituted hydroxyapa-tite and fluorapatite. J Mater Sci Mater Med 2003; 14:311-20; PMID:15348455; DOI:10.1023/A:1022975730730.
52. Catledge SA, Clem WC, Shrikishen N, Chowdhury S, Stanishevsky AV, Koopman M. An electrospun triphasic nanofibrous scaffold for bone tissue engineering. Biomed Mater 2007; 2:142-50; PMID:18458448; DOI:10.1088/1748-6041/2/2/013.
53. Itoh S, Kikuchi M, Koyama Y, Matumoto HN, Takakuda K, Shinomiya K. Development of a novel biomaterial, hydroxyapatite/collagen (HAp/Col) composite for medical use. J Biomed Mater Eng 2005; 15:29-41; PMID:15623928.
54. Masanori KB, Hiroko N, Matsumotob C, Takeki Y, Yoshihisa K, Kazuo T, et al. Glutaraldehyde cross-linked hydroxyapatite/collagen self-organized nanocomposites. Biomaterials 2004; 25:63-9; PMID:14580909; DOI:10.1016/S0142-9612(03)00472-1.
55. Teng S, Shi J, Peng BL, Chen F. The effect of alginate addition on the structure and morphology of hydroxyapatite/gelatin Nanocomposites. Compos Sci Technol 2006; 66:1532-8; DOI:10.1016/j.compscitech.2005.11.021.
56. Chang MC, Ko CC, Douglas WH. Conformational change of hydroxyapatite-gelatin nanocomposite by glutaraldehyde. Biomaterials 2003; 24:3087-94; PMID:12895581; DOI:10.1016/S0142-9612(03)00150-9.
57. Minfang C, Junjun T, Yuying L, Debao L. Preparation of Gelatin coated hydroxyapatite nanorods and the stability of its aqueous colloidal. Appl Surf Sci 2008; 254:2730-5; DOI:10.1016/j.apsusc.2007.10.011.
58. Kon E, Muraglia A, Corsi A. Electrospun poly(α-caprolactone)/gelatin nanofibrous scaffolds for nerve tissue engineering. J Biomed Mater Res 2000; 49:4532-9.
59. Barry FP, Murphy JM. Autologous bone marrow stromal cells loaded onto porous hydroxyapatite ceramic accelerate bone repair in critical-size defects of sheep long bones. Int J Biochem Cell Biol 2004; 36:328-37.
60. Wang YW, Wu Q, Chen GQ. Attachment, proliferation and differentiation of osteoblasts on random biopolyester poly(3-hydroxybutyrate-co-3-hydroxyhexanoate) scaffolds. Biomaterials 2004; 25:669-75; PMID:14607505; DOI:10.1016/S0142-9612(03)00561-1.
61. Morales JG, Burgues JT, Boix T, Fraile J, Clemente RR. Precipitation of Stoichiometric Hydroxyapatite by a Continuous Method. Cryst Res Technol 2001; 36:15-22; DOI:10.1002/1521-4079(200101)36:1<15::AID-CRAT15>3.0.CO;2-E.

©2011 Landes Bioscience. Do not distribute.